Nanoparticles

International Edition: DOI: 10.1002/anie.201606661
German Edition: DOI: 10.1002/ange.201606661

Fluorescent Gold Nanoclusters with Interlocked Staples and a Fully Thiolate-Bound Kernel

*Zibao Gan, Yuejian Lin, Lun Luo, Guangmei Han, Wei Liu, Zhengjie Liu, Chuanhao Yao, Linhong Weng, Lingwen Liao, Jishi Chen, Xu Liu, Yi Luo, Chengming Wang, Shiqiang Wei, and Zhikun Wu**

Abstract: *The structural features that render gold nanoclusters intrinsically fluorescent are currently not well understood. To address this issue, highly fluorescent gold nanoclusters have to be synthesized, and their structures must be determined. We herein report the synthesis of three fluorescent $Au_{24}(SR)_{20}$ nanoclusters ($R = C_2H_4Ph$, CH_2Ph, or $CH_2C_6H_4{}^tBu$). According to UV/Vis/NIR, differential pulse voltammetry (DPV), and X-ray absorption fine structure (XAFS) analysis, these three nanoclusters adopt similar structures that feature a bi-tetrahedral Au_8 kernel protected by four tetrameric $Au_4(SR)_5$ motifs. At least two structural features are responsible for the unusual fluorescence of the $Au_{24}(SR)_{20}$ nanoclusters: Two pairs of interlocked $Au_4(SR)_5$ staples reduce the vibration loss, and the interactions between the kernel and the thiolate motifs enhance electron transfer from the ligand to the kernel moiety through the Au–S bonds, thereby enhancing the fluorescence. This work provides some clarification of the structure–fluorescence relationship of such clusters.*

Fluorescent noble-metal nanoclusters (NCs) that consist of several to hundreds of metal atoms have recently attracted extensive interest and have emerged as a novel type of fluorescent nanomaterial not only for fundamental scientific research but also for practical applications because of their well-defined composition (structure) and various beneficial properties (such as the ultrasmall size, excellent biocompatibility, and high surface tunability).[1–12] The first attribute (well-defined composition and structure), in particular, provides an opportunity for investigating the origin of the fluorescence of nanoclusters, which is difficult for larger fluorescent nanoparticles owing to their polydispersity and undefined structures.[13–18] After continuous efforts, some insight into the origin of the fluorescence of such nanoparticles has recently been gained.[19–26] For example, Wu and Jin showed that the fluorescence of gold nanoclusters is sensitive to the ligands and the electropositivity of the gold core.[20] Xie et al. suggested an aggregation induced emission (AIE) mechanism.[24] These proposals provide a rational interpretation for the fluorescence of some nanoclusters, especially for nanoclusters with hydrophilic ligands such as DNA,[27,28] dendrimers,[22,29] or peptides.[30,31] However, they cannot explain the more recently discovered strong fluorescence of Au_{24} clusters protected with hydrophobic phenylethanethiolate.[32] The influence of the nanocluster structure on the fluorescence was likely not fully understood in the previous proposals. Unfortunately, the structure of $Au_{24}(SC_2H_4Ph)_{20}$ was unknown at that time, which impeded the analysis. Although the structures of selenolate- and 4-*tert*-butylbenzylmercaptan-capped Au_{24} nanoclusters have been known for some time,[33,34] the structure of $Au_{24}(SC_2H_4Ph)_{20}$ cannot be simply assigned to either one because of their structural differences and possible isomerism.[35] For several years, we have tried to grow high-quality single crystals of $Au_{24}(SC_2H_4Ph)_{20}$; unfortunately, our efforts have not been successful to date. As a result, we have turned our attention to determine the structure of other Au_{24} nanoclusters. Regrettably, a previously reported synthetic method[32] is not applicable to the synthesis of other Au_{24} nanoclusters protected with a homologous ligand (e.g., $HSCH_2Ph$). The development of a universal, facile method to synthesize Au_{24} nanoclusters protected by various ligands would be of great importance for structure deduction and in-depth structure–fluorescence relationship studies. Herein, we introduce such a method to synthesize $Au_{24}(SR)_{20}$ ($R = C_2H_4Ph$, CH_2Ph, or $CH_2C_6H_4{}^tBu$) nanoclusters. We also determined the structure of $Au_{24}(SCH_2Ph)_{20}$ and $Au_{24}(SCH_2C_6H_4{}^tBu)_{20}$ by single-crystal

[*] Z. Gan, C. Yao, L. Liao, J. Chen, X. Liu, Prof. Z. Wu
Key Laboratory of Materials Physics
Anhui Key Laboratory of Nanomaterials and Nanostructures
Institute of Solid State Physics
Chinese Academy of Sciences, Hefei, 230031 (China)
E-mail: zkwu@issp.ac.cn

Y. Lin, L. Weng
Shanghai Key Laboratory of Molecular Catalysis and Innovative Materials, Department of Chemistry, Fudan University
Shanghai, 200433 (China)

L. Luo, Y. Luo
State Key Laboratory of Fine Chemicals
School of Pharmaceutical Science and Technology
Dalian University of Technology
Dalian, 116024 (China)

G. Han, Z. Liu
Institute of Intelligent Machines
Chinese Academy of Sciences
Hefei, 230031 (China)

W. Liu, S. Wei
National Synchrotron Radiation Facility
University of Science and Technology of China
Hefei, 230029 (China)

C. Wang
Hefei National Laboratory for Physical Sciences at the Microscale
University of Science and Technology of China
Hefei, 230026 (China)

Supporting information for this article can be found under: http://dx.doi.org/10.1002/anie.201606661.

X-ray crystallography, and investigated the influence of the nanocluster structure on the fluorescence.

To synthesize $Au_{24}(SCH_2Ph)_{20}$ nanoclusters, for example, $Au_{25}(SC_2H_4Ph)_{18}$ nanoclusters (10 mg) were dissolved in a solution of dichloromethane (DCM, 1 mL) and $PhCH_2SH$ (0.25 mL; for details, see the Supporting Information, Figure S1). Next, the reaction mixture was stirred at room temperature for 18 h, and the reaction was then terminated by the addition of a large amount of methanol. The precipitates were washed with methanol three times, dissolved in DCM, and then separated and purified by preparative thin-layer chromatography (PTLC). Single crystals of the purified nanoclusters were obtained by dissolving $Au_{24}(SCH_2Ph)_{20}$ nanoclusters in DCM, followed by vapor diffusion of pentane into the nanocluster solution. Orange crystals were obtained after one to two days. The composition of the $Au_{24}(SC_2H_4Ph)_{20}$ nanoclusters was confirmed by electrospray ionization mass spectrometry (ESI-MS); CsOAc was added to the nanocluster solution to form $[cluster+xCs]^{x+}$ adducts before ESI-MS analysis. As shown in Figure 1, two intense

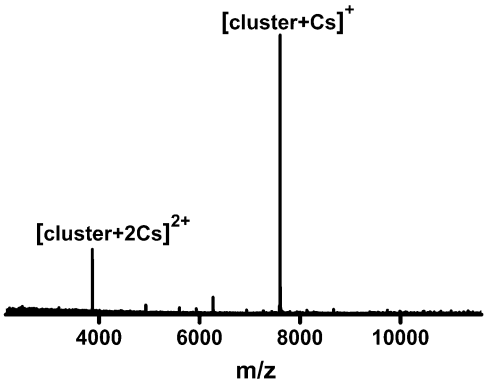

Figure 1. ESI-MS spectrum (positive-ion mode) of $Au_{24}(SC_2H_4Ph)_{20}$.

peaks at m/z 7605.0 and 3869.5 were observed, which were readily assigned to $[Au_{24}(SC_2H_4Ph)_{20}Cs]^+$ (calcd: 7604.96, deviation: 0.04) and $[Au_{24}(SC_2H_4Ph)_{20}Cs_2]^{2+}$ (calcd: 3869.44, deviation: 0.06), respectively. The as-obtained nanoclusters are thus composed of 24 gold atoms and 20 phenylethanethiolates ($Au_{24}(SC_2H_4Ph)_{20}$), the same nanoclusters as in our previous report,[32] as further confirmed by a comparison of their absorption spectra (Figure S2). The absorption bands of the phenylmethanethiolated and 4-*tert*-butylphenylmethanethiolated nanoclusters are very similar to those of $Au_{24}(SC_2H_4Ph)_{20}$, except for some slight red shifts, indicating that the three nanoclusters have similar compositions and structures. This hypothesis was further supported by their almost identical electrochemical properties (Figure 2) and X-ray absorption fine structure (XAFS)[36] analysis (Figure S3). Thermogravimetric analysis revealed a weight loss of 42.7% (see Figure S4) for the 4-*tert*-butylphenylmethanethiolated nanoclusters, which is in perfect agreement with the theoretical value of $Au_{24}(SCH_2C_6H_4{}^tBu)_{20}$ (43.1%). Furthermore, their absorption spectrum is also identical to that of previously reported $Au_{24}(SCH_2C_6H_4{}^tBu)_{20}$ (see Figure S5).[34] Single-crystal X-ray crystallography unambiguously con-

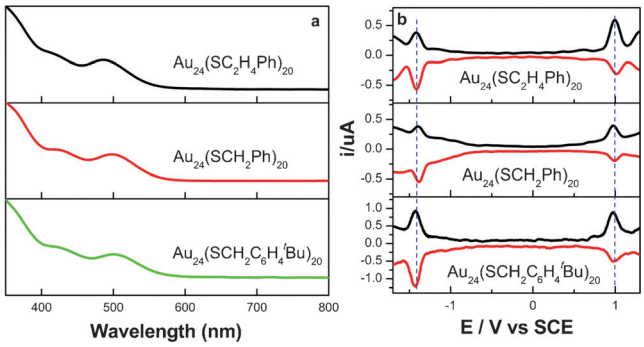

Figure 2. a) UV/Vis/NIR spectra and b) DPV curves of $Au_{24}(SC_2H_4Ph)_{20}$, $Au_{24}(SCH_2Ph)_{20}$, and $Au_{24}(SCH_2C_6H_4{}^tBu)_{20}$ nanocluster solutions in DCM.

firmed the compositions of the phenylmethanethiolated and 4-*tert*-butylbenzylmethanethiolated nanoclusters to be $Au_{24}(SCH_2Ph)_{20}$ and $Au_{24}(SCH_2C_6H_4{}^tBu)_{20}$, respectively. Their structures (Figure 3 and Figure S6) are similar to a previously

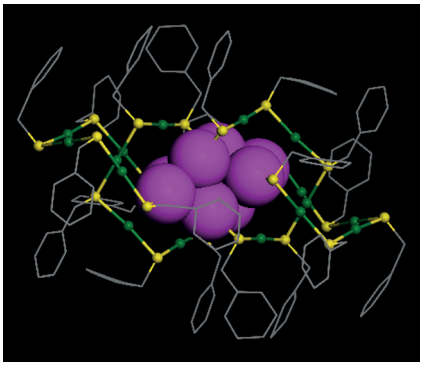

Figure 3. Crystal structure of the $Au_{24}(SCH_2Ph)_{20}$ nanocluster with the Au_8 kernel shown in space-filling form, the surface-protecting motifs in ball-and-stick form, and the carbon tails in wireframe form.

reported structure of $Au_{24}(SCH_2C_6H_4{}^tBu)_{20}$,[34] but distinctly different from that of $Au_{24}(SePh)_{20}$.[33] $Au_{24}(SCH_2Ph)_{20}$, for example, is composed of a bi-tetrahedral Au_8 kernel (Figure 4a) with an fcc-based antiprismatic shape and two pairs of tetrameric staples ($Au_4(SCH_2Ph)_5$; Figure 4e) that protect the Au_8 kernel. The $Au_4(SCH_2Ph)_5$ tetramers adopt a chair-like conformation and are attached to two Au atoms of one kernel tetrahedron through bidentate ligation (Figures 4b–e).

As revealed previously,[32] the fluorescence of $Au_{24}(SC_2H_4Ph)_{20}$ is indeed superior to that of the common $Au_n(SR)_m$ nanoclusters protected by hydrophobic ligands,[37–42] as shown in Figure 5a. Red fluorescence has been reported for gold nanoclusters several times before;[32,34,43–45] for example, Chang et al. reported that dihydrolipoic acid protected gold nanoclusters displayed an emission maximum at 700 nm.[43] However, some Au clusters with green or blue fluorescence have also been described.[44,46–50] This discrepancy could be due to the fact that the emission wavelength of gold nanoclusters is influenced by multiple factors such as the protecting ligands[46,48] and the

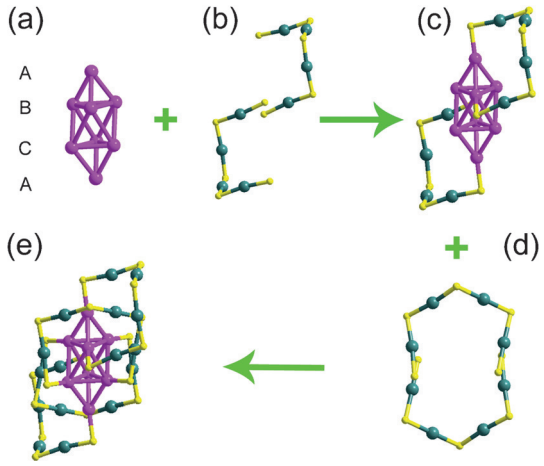

Figure 4. Analysis of the $Au_{24}(SCH_2Ph)_{20}$ nanocluster structure. The addition of one pair of $Au_4(SCH_2Ph)_5$ staples (b) to an fcc Au_8 kernel (a) gives rise to the structure shown in (c). The addition of another pair of $Au_4(SCH_2Ph)_5$ staples (d) then leads to $Au_{24}(SCH_2Ph)_{20}$ (e). Au in the kernel: magenta, Au on the surface: teal, S: yellow.

nanocluster size.[44,48] Knowing the structures of $Au_{24}(SCH_2Ph)_{20}$ and $Au_{24}(SCH_2C_6H_4{}^tBu)_{20}$ paves the way for an analysis of the structure–fluorescence correlation of $Au_{24}(SC_2H_4Ph)_{20}$ because it has been deduced that $Au_{24}(SC_2H_4Ph)_{20}$ adopts a similar structure to $Au_{24}(SCH_2Ph)_{20}$ or $Au_{24}(SCH_2C_6H_4{}^tBu)_{20}$, as discussed above. For comparison, the structures of the $Au_{24}(SR)_{20}$ nanoclusters described in this manuscript and other common $Au_n(SR)_m$ nanoclusters protected by hydrophobic ligands[37–42] are shown in Figure 5b. Structures with different numbers of Au atoms are displayed to make it clear that the fluorescence of gold nanoclusters is not exclusively determined by the amount of Au in the nanocluster. One obvious structural feature of $Au_{24}(SR)_{20}$ is that it contains two pairs of interlocked $Au_4(SR)_5$ staples; another feature is that all eight gold atoms in the Au_8 kernel are fully bound to the sulfur atoms of thiolates through Au–S bonds. As expected, these two structural features promote the emission. The first feature increases the rigidity of the whole nanocluster and reduces the emission loss by vibration;[25] the latter affects the interaction between the kernel and the thiolates and strengthens the electron transfer from the ligands to the kernel through the Au–S bonds, thereby increasing the fluorescence, as previously described by us.[20]

Herein, we further demonstrate that the electron transfer from the ligand to the kernel plays a vital role in triggering the fluorescence of the nanoclusters: When the SC_2H_4Ph group was replaced by SCH_2Ph or even $SCH_2C_6H_4{}^tBu$, the fluorescence of the corresponding nanocluster becomes more intense (Figure 6) with an increase in the electron-donor strength of the thiolate (the fluorescence quantum yields of $Au_{24}(SC_2H_4Ph)_{20}$, $Au_{24}(SCH_2Ph)_{20}$, and $Au_{24}(SCH_2C_6H_4{}^tBu)_{20}$ are 0.3, 1.5, 2%, respectively, calibrated to $Au_{22}(SG)_{18}$;[45] see Figure S7). Theoretical calculations also revealed that the overall Hirshfeld charge[51] of the Au atoms in the Au_8 kernel is 0.28 in $Au_{24}(SCH_2Ph)_{20}$ and 0.32 in $Au_{24}(SCH_2C_6H_4{}^tBu)_{20}$, which indicates that the Au_8 kernel in $Au_{24}(SCH_2C_6H_4{}^tBu)_{20}$ attracts the delocalized electrons more strongly than that in $Au_{24}(SCH_2Ph)_{20}$. The fact that $Au_{24}(SePh)_{20}$ does not fluoresce provides additional evidence for this hypothesis because the electron transfer through Au–Se bonds is more difficult than transfer through Au–S bonds (Figure 6).

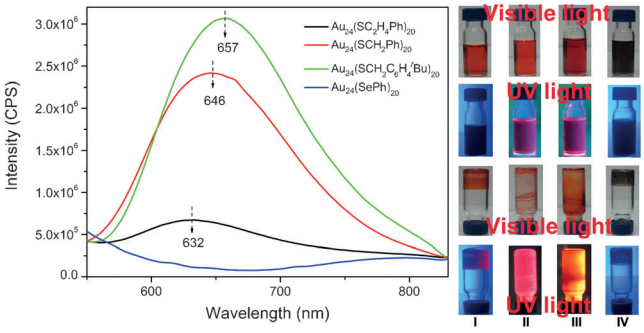

Figure 6. Fluorescence spectra of $Au_{24}(SC_2H_4Ph)_{20}$, $Au_{24}(SCH_2Ph)_{20}$, $Au_{24}(SCH_2C_6H_4{}^tBu)_{20}$, and $Au_{24}(SePh)_{20}$ nanoclusters dissolved in DCM (left) and digital photographs (I–IV) under visible and 365 nm UV light irradiation (right).

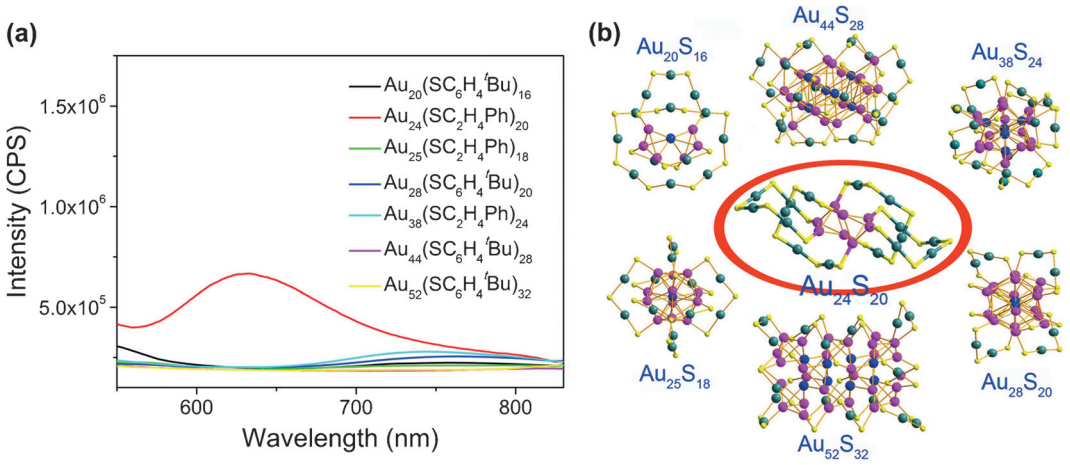

Figure 5. a) Fluorescence spectra and b) structural frameworks of various Au nanoclusters (for convenience, all R groups were replaced by "S"). Au in the kernel and bound to S: magenta, Au in the kernel and not bound to S: blue, Au on the surface: teal, S: yellow.

Briefly, the extensive fluorescence of $Au_{24}(SR)_{20}$ nanoclusters can be attributed to their structure with interlocked staples and a fully thiolate-bound kernel core. Interestingly, the strongly fluorescent $Au_{22}(SG)_{18}$ nanoclusters recently reported by Xie et al. share these structural features,[45] which provides additional support for our proposal on the structure–fluorescence correlation. The three clusters, especially those with relatively strong fluorescence ($Au_{24}(SCH_2Ph)_{20}$ and $Au_{24}(SCH_2C_6H_4{}^tBu)_{20}$) are somewhat stable in mildly reducing environments while they decompose under harsh conditions (see Figures S8–S13). The fluorescence quantum yields of the three clusters are not very high compared with those of some previously reported compounds,[52–56] but they could be greatly improved. For instance, the fluorescence quantum yield of $Au_{24}(SCH_2C_6H_4{}^tBu)_{20}$ could be increased to 7.6% (or 9.8%; Figures S14 and S15) by ligand exchange using 11-mercaptoundecanoic acid (or mercapto-containing bovine serum albumin, BSA) as the incoming ligand (see the Supporting Information for details). Taken together, these facts indicate potential applications of such structured gold nanoclusters. The BSA-exchanged $Au_{24}(SCH_2C_6H_4{}^tBu)_{20}$ nanoclusters were indeed used for the imaging of living macrophages, and the negligible cytotoxicity of the labeling reagent under the investigated conditions was confirmed in a 3-(4,5-dimethylthiazol-2-yl)-2,5-diphenyltetrazolium bromide (MTT) assay (Figure 7). Notably, other thiolated nanoclusters have also been successfully used in complex bioenvironments.[8,11,43,57,58]

In summary, we have described a universal route for the facile synthesis of fluorescent $Au_{24}(SR)_{20}$ nanoclusters. UV/Vis/NIR, DPV, and XAFS analysis indicated that $Au_{24}(SC_2H_4Ph)_{20}$ clusters adopt a similar structure to $Au_{24}(SCH_2Ph)_{20}$ and $Au_{24}(SCH_2C_6H_4{}^tBu)_{20}$, and feature a bi-tetrahedral Au_8 kernel that is protected by four tetrameric $Au_4(SR)_5$ motifs. The thiolated Au_{24} nanoclusters exhibit bright red photoluminescence, and the fluorescence intensity increases with an increase in the electron-donor strength of the ligand. Compared with some other common nanoclusters protected by hydrophobic ligands, the three Au_{24} nanoclusters reported herein exhibit unusually strong fluorescence owing to their particular structures. The interlocked $Au_4(SR)_5$ staples reduce the emission loss by vibration, and the interactions between the kernel and the thiolates strengthen the electron transfer from the thiolates to the kernel through the Au–S bonds, thus leading to enhanced fluorescence. We believe that our work has important implications for structure–fluorescence relationship studies and will provide some guidance for the synthesis and application, for example, in bioimaging, of novel fluorescent nanoclusters.

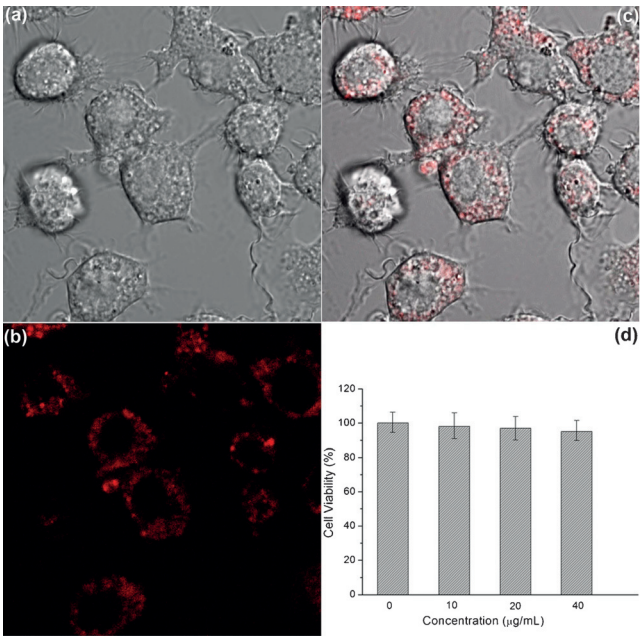

Figure 7. Laser confocal images of macrophages after incubation with BSA-exchanged $Au_{24}(SCH_2C_6H_4{}^tBu)_{20}$ for 4 h. a) Bright-field image, b) excitation at 488 nm, and c) merged image. d) Viability of the macrophages after 24 h incubation with various concentrations of BSA-exchanged $Au_{24}(SCH_2C_6H_4{}^tBu)_{20}$ nanoclusters.

Acknowledgements

We thank the Natural Science Foundation of China (21222301, 21528303, 21171170, 51502299), the Postdoctoral Science Foundation of China (2015M571951), the National Basic Research Program of China (2013CB934302), the Ministry of Human Resources and Social Security of China, the Innovative Program of Development Foundation of Hefei Centre for Physical Science and Technology (2014FXCX002), the Hefei Science Center, CAS (2015HSC-UP003), the CAS/SAFEA International Partnership Program for Creative Research Teams, and the Hundred Talents Program of the Chinese Academy of Sciences for financial support.

Keywords: fluorescence · gold · nanoclusters · synthetic methods

How to cite: *Angew. Chem. Int. Ed.* **2016**, *55*, 11567–11571
Angew. Chem. **2016**, *128*, 11739–11743

[1] J. Xie, Y. Zheng, J. Y. Ying, *J. Am. Chem. Soc.* **2009**, *131*, 888.
[2] Y. Lu, W. Chen, *Chem. Soc. Rev.* **2012**, *41*, 3594.
[3] J. Guo, S. Kumar, M. Bolan, A. Desireddy, T. P. Bigioni, W. P. Griffith, *Anal. Chem.* **2012**, *84*, 5304.
[4] Z. Wu, M. Wang, J. Yang, X. Zheng, W. Cai, G. Meng, H. Qian, H. Wang, R. Jin, *Small* **2012**, *8*, 2028.
[5] M. Ganguly, J. Pal, S. Das, C. Mondal, Y. Negishi, T. Pal, *Langmuir* **2013**, *29*, 10945.
[6] S. H. Yau, O. Varnavski III, T. Goodson, *Acc. Chem. Res.* **2013**, *46*, 1506.
[7] L. Zhang, E. Wang, *Nano Today* **2014**, *9*, 132.
[8] S. Wang, X. Meng, A. Das, T. Li, Y. Song, T. Cao, X. Zhu, M. Zhu, R. Jin, *Angew. Chem. Int. Ed.* **2014**, *53*, 2376; *Angew. Chem.* **2014**, *126*, 2408.
[9] I. Chakraborty, R. G. Bhuin, S. Bhat, T. Pradeep, *Nanoscale* **2014**, *6*, 8561.
[10] X. Wan, W. Xu, S. Yuan, Y. Gao, X. Zeng, Q. Wang, *Angew. Chem. Int. Ed.* **2015**, *54*, 9683; *Angew. Chem.* **2015**, *127*, 9819.
[11] J. Yang, N. Xia, X. Wang, X. Liu, A. Xu, Z. Wu, Z. Luo, *Nanoscale* **2015**, *7*, 18464.
[12] M. S. Bootharaju, C. P. Joshi, M. R. Parida, O. F. Mohammed, O. M. Bark, *Angew. Chem. Int. Ed.* **2016**, *55*, 922; *Angew. Chem.* **2016**, *128*, 934.

[13] S. Dolai, P. R. Nimmmala, M. Mandal, B. B. Muhoberac, K. Dria, A. Dass, R. Sardar, *Chem. Mater.* **2014**, *26*, 1278.
[14] K. Dohnalová, A. N. Poddubny, A. A. Prokofiev, W. D. A. M. de Boer, C. P. Umesh, J. M. J. Paulusse, H. Zuilhof, T. Gregorkiewicz, *Light: Sci. Appl.* **2013**, *2*, e47.
[15] S. K. Das, Y. Liu, S. Yeom, D. Y. Kim, C. I. Richards, *Nano Lett.* **2014**, *14*, 620.
[16] K. Dohnalová, T. Gregorkiewicz, K. Kusova, *J. Phys. Condens. Matter* **2014**, *26*, 173201.
[17] J. B. Miller, N. Dandu, K. A. Velizhanin, R. J. Anthony, U. R. Kortshagen, D. M. Kroll, A. S. Kilin, E. K. Hobbie, *ACS Nano* **2015**, *9*, 9772.
[18] S. Khan, N. C. Verma, A. Gupta, C. K. Nandi, *Sci. Rep.* **2015**, *5*, 11423.
[19] G. Wang, T. Huang, R. W. Murray, L. Menard, R. G. Nuzzo, *J. Am. Chem. Soc.* **2005**, *127*, 812.
[20] Z. Wu, R. Jin, *Nano Lett.* **2010**, *10*, 2568.
[21] S. H. Yau, O. Varnavski, J. D. Gilbertson, B. Chandler, G. Ramakrishna II, T. Goodson, *J. Phys. Chem. C* **2010**, *114*, 15979.
[22] Y. Chen, T. Yang, H. Pan, Y. Yuan, L. Chen, M. Liu, K. Zhang, S. Zhang, P. Wu, J. Xu, *J. Am. Chem. Soc.* **2014**, *136*, 1686.
[23] T. D. Green, C. Yi, C. Zeng, R. Jin, S. McGill, K. L. Knappenberger, Jr., *J. Phys. Chem. A* **2014**, *118*, 10611.
[24] Z. Luo, X. Yuan, Y. Yu, Q. Zhang, D. T. Leong, J. Y. Lee, J. Xie, *J. Am. Chem. Soc.* **2012**, *134*, 16662.
[25] K. Pyo, V. D. Thanthirige, K. Kwak, P. Pandurangan, G. Ramakrishna, D. Lee, *J. Am. Chem. Soc.* **2015**, *137*, 8244.
[26] B. A. Ashenfelter, A. Desireddy, S. H. Yau III, T. Goodson, T. P. Bigioni, *J. Phys. Chem. C* **2015**, *119*, 20728.
[27] R. Zhou, M. Shi, X. Chen, M. Wang, H. Chen, *Chem. Eur. J.* **2009**, *15*, 4944.
[28] L. Zhang, J. Zhu, Z. Zhou, S. Guo, J. Li, S. Dong, E. Wang, *Chem. Sci.* **2013**, *4*, 4004.
[29] I. Díez, M. I. Kanyuk, A. P. Demchenko, A. Walther, H. Jiang, O. Ikkala, R. H. A. Ras, *Nanoscale* **2012**, *4*, 4434.
[30] Y. Yu, S. Y. New, J. Xie, X. Su, Y. N. Tan, *Chem. Commun.* **2014**, *50*, 13805.
[31] A. Baksi, M. S. Bootharaju, X. Chen, H. Häkkinen, T. Pradeep, *J. Phys. Chem. C* **2014**, *118*, 21722.
[32] C. Yao, S. Tian, L. Liao, X. Liu, N. Xia, N. Yan, Z. Gan, Z. Wu, *Nanoscale* **2015**, *7*, 16200.
[33] Y. Song, S. Wang, J. Zhang, X. Kang, S. Chen, P. Li, H. Sheng, M. Zhu, *J. Am. Chem. Soc.* **2014**, *136*, 2963.
[34] A. Das, T. Li, G. Li, K. Nobusada, C. Zeng, N. L. Rosi, R. Jin, *Nanoscale* **2014**, *6*, 6458.
[35] S. Tian, Y. Li, M. Li, J. Yuan, J. Yang, Z. Wu, R. Jin, *Nat. Commun.* **2015**, *6*, 8667.
[36] L. Yang, H. Cheng, Y. Jiang, T. Huang, J. Bao, Z. Sun, Z. Jiang, J. Ma, F. Sun, Q. Liu, T. Yao, H. Deng, S. Wang, M. Zhu, S. Wei, *Nanoscale* **2015**, *7*, 14452.
[37] C. Zeng, C. Liu, Y. Chen, N. L. Rosi, R. Jin, *J. Am. Chem. Soc.* **2014**, *136*, 11922.
[38] M. W. Heaven, A. Dass, P. S. White, K. M. Holt, R. W. Murray, *J. Am. Chem. Soc.* **2008**, *130*, 3754.
[39] C. Zeng, T. Li, A. Das, N. L. Rosi, R. Jin, *J. Am. Chem. Soc.* **2013**, *135*, 10011.
[40] H. Qian, W. T. Eckenhoff, Y. Zhu, T. Pintauer, R. Jin, *J. Am. Chem. Soc.* **2010**, *132*, 8280.
[41] C. Zeng, Y. Chen, K. Lida, K. Nobusada, K. Kirschbaum, K. J. Lambright, R. Jin, *J. Am. Chem. Soc.* **2016**, *138*, 3850.
[42] C. Zeng, Y. Chen, C. Liu, K. Nobusada, N. L. Rosi, R. Jin, *Sci. Adv.* **2015**, *1*, e1500425.
[43] C. J. Lin, T. Yang, C. Lee, S. H. Huang, R. A. Sperling, M. Zanella, J. K. Li, J. Shen, H. Wang, H. I. Yeh, W. J. Parak, W. H. Chang, *ACS Nano* **2009**, *3*, 395.
[44] J. Zheng, P. R. Nicovich, R. M. Dickson, *Annu. Rev. Phys. Chem.* **2007**, *58*, 409.
[45] Y. Yu, Z. Luo, D. M. Chevrier, D. T. Leong, P. Zhang, D. Jiang, J. Xie, *J. Am. Chem. Soc.* **2014**, *136*, 1246.
[46] C. C. Huang, Z. Yang, K. H. Lee, H. T. Chang, *Angew. Chem. Int. Ed.* **2007**, *46*, 6824; *Angew. Chem.* **2007**, *119*, 6948.
[47] H. Zhu, T. Yu, H. Xu, K. Zhang, H. Jiang, Z. Zhang, Z. Wang, S. Wang, *ACS Appl. Mater. Interfaces* **2014**, *6*, 21461.
[48] H. Jiang, Y. Zhang, X. Wang, *Nanoscale* **2014**, *6*, 10355.
[49] P. Khandelwal, D. K. Singh, S. Sadhu, P. Poddar, *Nanoscale* **2015**, *7*, 19985.
[50] Z. Wang, W. Cai, J. Sui, *ChemPhysChem* **2009**, *10*, 2012.
[51] R. F. Nalewajski, R. G. Parr, *Proc. Natl. Acad. Sci. USA* **2000**, *97*, 8879.
[52] I. L. Volkov, P. Y. Serdobintsev, A. I. Kononov, *J. Phys. Chem. C* **2013**, *117*, 24079.
[53] M. Tang, D. P. Tsang, Y. Wong, M. Chan, K. M. Wong, V. W. Yam, *J. Am. Chem. Soc.* **2014**, *136*, 17861.
[54] Y. Bekenstein, B. A. Koscher, S. W. Eaton, P. Yang, A. P. Alivisatos, *J. Am. Chem. Soc.* **2015**, *137*, 16008.
[55] Y. Kong, J. Chen, H. Fang, G. Heath, Y. Wo, W. Wang, Y. Li, Y. Gao, S. D. Evans, S. Chen, *Chem. Mater.* **2016**, *28*, 3041.
[56] J. Dong, X. Song, Y. Shi, Z. Gao, B. Li, N. Li, H. Luo, *Biosens. Bioelectron.* **2016**, *81*, 473.
[57] X. Zhang, F. Wu, P. Liu, N. Gu, Z. Chen, *Small* **2014**, *10*, 5170.
[58] M. A. H. Muhammed, P. K. Verma, S. K. Pal, R. C. A. Kumar, S. Paul, R. V. Omkumar, T. Pradeep, *Chem. Eur. J.* **2009**, *15*, 10110.

Received: July 9, 2016
Published online: August 16, 2016

